Experimental Eye Research 107 (2013) 21–31

Contents lists available at SciVerse ScienceDirect

Experimental Eye Research

journal homepage: www.elsevier.com/locate/yexer

Sigma-1 receptor stimulation attenuates calcium influx through activated L-type Voltage Gated Calcium Channels in purified retinal ganglion cells

Brett H. Mueller II [a,c], Yong Park [a,c], Donald R. Daudt III [a,c], Hai-Ying Ma [a,c], Irina Akopova [d], Dorota L. Stankowska [b,c], Abbot F. Clark [b,c], Thomas Yorio [a,c,*]

[a] Department of Pharmacology and Neuroscience, University of North Texas Health Science Center, Fort Worth, TX, USA
[b] Department of Cell Biology and Anatomy, University of North Texas Health Science Center, Fort Worth, TX, USA
[c] North Texas Eye Research Institute, University of North Texas Health Science Center, Fort Worth, TX, USA
[d] Department of Molecular Biology and Immunology, Center for Commercialization of Fluorescence Technologies, University of North Texas Health Science Center, Fort Worth, TX, USA

ARTICLE INFO

Article history:
Received 21 May 2012
Accepted in revised form 7 November 2012
Available online 23 November 2012

Keywords:
purified retinal ganglion cells
L-type Voltage Gated Calcium Channel
calcium signaling
sigma-1 receptor

ABSTRACT

Sigma-1 receptors (σ-1rs) exert neuroprotective effects on retinal ganglion cells (RGCs) both *in vivo* and *in vitro*. This receptor has unique properties through its actions on several voltage-gated and ligand-gated channels. The purpose of this study was to investigate the role that σ-1rs play in regulating cell calcium dynamics through activated L-type Voltage Gated Calcium Channels (L-type VGCCs) in purified RGCs. RGCs were isolated from P3-P7 Sprague–Dawley rats and purified by sequential immunopanning using a Thy1.1 antibody. Calcium imaging was used to measure changes in intracellular calcium after depolarizing the cells with potassium chloride (KCl) in the presence or absence of two σ-1r agonists [(+)-SKF10047 and (+)-Pentazocine], one σ-1r antagonist (BD1047), and one L-type VGCC antagonist (Verapamil). Finally, co-localization studies were completed to assess the proximity of σ-1r with L-type VGCCs in purified RGCs. VGCCs were activated using KCl (20 mM). Pre-treatment with a known L-type VGCC blocker demonstrated a 57% decrease of calcium ion influx through activated VGCCs. Calcium imaging results also demonstrated that σ-1r agonists, (+)-N-allylnormetazocine hydrochloride [(+)-SKF10047] and (+)-Pentazocine, inhibited calcium ion influx through activated VGCCs. Antagonist treatment using BD1047 demonstrated a potentiation of calcium ion influx through activated VGCCs and abolished all inhibitory effects of the σ-1r agonists on VGCCs, implying that these ligands were acting through the σ-1r. An L-type VGCC blocker (Verapamil) also inhibited KCl activated VGCCs and when combined with the σ-1r agonists there was not a further decline in calcium entry suggesting similar mechanisms. Lastly, co-localization studies demonstrated that σ-1rs and L-type VGCCs are co-localized in purified RGCs. Taken together, these results indicated that σ-1r agonists can inhibit KCl induced calcium ion influx through activated L-type VGCCs in purified RGCs. This is the first report of attenuation of L-type VGCC signaling through the activation of σ-1rs in purified RGCs. The ability of σ-1rs to co-localize with L-type VGCCs in purified RGCs implied that these two proteins are in close proximity to each other and that such interactions regulate L-type VGCCs.

1. Introduction

The sigma-1 receptor (σ-1r) is a 26 kDa protein that was once categorized as an opioid receptor (Martin et al., 1976; Hanner et al., 1996). However, further studies have demonstrated that this receptor is a unique non-opioid receptor with separate pharmacological properties including the ability to bind to benzomorphans (e.g. (+)-pentazocine and (+)-SKF10047), steroids (e.g. progesterone and testosterone) and psychotropic drugs (e.g. haloperidol) (Hayashi and Su, 2005). There appear to be several subtypes of sigma receptors (σ-1r and σ-2r, and σ-3r) (Quirion et al., 1992; Myers et al., 1994), but σ-1r is the only receptor that has been

Abbreviations: KCl, Potassium Chloride; σ-1r, sigma-1 receptor; VGCCs, Voltage Gated Calcium Channels; L-type VGCCs, L-type Voltage Gated Calcium Channels; RGCs, Retinal Ganglion Cells; ER, endoplasmic reticulum; TIFRM, Total Internal Reflection Fluorescence Microscopy; EFF, evanescent field fluorescence; $[Ca^{2+}]_i$, cytoplasmic calcium concentration.

* Corresponding author. Department of Pharmacology and Neuroscience, University of North Texas Health Science Center, 3500 Camp Bowie Blvd., Fort Worth, TX 76107, USA. Tel.: +1 817 735 2068; fax: +1 817 735 2419.
E-mail addresses: bmueller@live.unthsc.edu (B.H. Mueller), yoriot@hsc.unt.edu, Thomas.Yorio@unthsc.edu (T. Yorio).

0014-4835
http://dx.doi.org/10.1016/j.exer.2012.11.002

cloned and characterized in several animal species (Hanner et al., 1996; Kekuda et al., 1996; Seth et al., 1997, 1998). The endogenous ligand and function of σ-1r is not yet known. This receptor has been shown to be predominantly localized on the endoplasmic reticulum (ER), with two transmembrane spanning regions, that possess the ability to translocate to the plasma membrane upon agonist stimulation or under prolonged stress (Hayashi and Su, 2003; Aydar et al., 2002). The translocation of σ-1r to the plasma membrane is thought to be the mechanism underlying the ability of an ER protein like σ-1r to modulate and regulate many different ion channels on the plasma membrane including voltage-gated and ligand-gated Ca^{2+}, K^{+}, Na^{+}, Cl^{-}, and SK ion channels (Hayashi and Su, 2003; Aydar et al., 2002; Maurice and Su, 2009; Su et al., 2009).

A number of studies have suggested that σ-1r ligands regulate the activity of voltage gated calcium channels (VGCCs). For instance, Zhang and Cuevas (2002) demonstrated in parasympathetic and sympathetic primary neuronal cultures that σ-1r ligand compounds can facilitate calcium current inactivation of L-, N-, P/Q-, and R-type VGCCs. In primary hippocampal neurons, Church and Fletcher (1995) also demonstrated that σ-1r ligands block multiple subtypes of VGCC currents. Hayashi et al. (2000) and Tchedre et al. (2008) demonstrated in neuronal cell lines that σ-1r agonist stimulation also diminished calcium ion influx through activated VGCCs.

To date, there have been no reported studies demonstrating σ-1r modulatory effects on any ligand gated ion channels or VGCCs in purified retinal ganglion cells (RGCs). Only one study has demonstrated an inhibitory effect of σ-1r agonist stimulation on NMDA induced calcium ion influx in retinal cross-sections (Zhang et al., 2011). Therefore, it was important to investigate the role that σ-1r and σ-1r ligands play in regulating calcium ion influx in purified RGCs.

In this study, we used purified RGC cultures to study the effects of two σ-1r agonists (SKF10047 and Pentazocine) and one σ-1r antagonist (BD1047) on activated VGCCs in purified RGCs. The goal of this study was to evaluate pharmacologically if σ-1r ligands act through the σ-1r to attenuate or potentiate calcium ion influx through activated VGCCs. Lastly, this study aims to identify the subtype of VGCC that σ-1r ligand mediated effects occur in purified RGCs.

2. Materials and methods

2.1. Primary RGC isolation

All procedures were performed in accordance with the ARVO Statement for the Use of Animals in Ophthalmic and Vision Research and were approved by the Institutional Animal Care and Use Committee (IACUC) at the University of North Texas Health Science Center. Dr. Ben Barres trained our laboratory to perform his two-step panning purified retinal ganglion cell isolation (Christopherson et al., 2005; Meyer et al., 1995; Ullian et al., 2001; Barres et al., 1988). Purity utilizing this method has been described at 96%–99.5% (Christopherson et al., 2005; Meyer et al., 1995; Ullian et al., 2001; Barres et al., 1988). We found our isolation procedure resulted in a greater than 98% purity as seen using appropriate cell markers.

Sprague Dawley rats (post-natal day 3–7) (Charler River, Wilmington, MA) were euthanized, and the retinas were placed in 4.5 units/mL of papain solution (Worthington, Lakewood, NJ) to dissociate the cells. Cells were then incubated for 10 min with a rabbit anti-macrophage antibody (Cedarlane, Burlington, Ontario, Canada). Cell suspensions were then incubated in a 150-mm petri dish coated with a goat anti-rabbit IgG (H + L chain) antibody (Jackson ImmunoResearch, West Grove, PA) for 30 min. Cells that did not adhere to the 150-mm dish were then transferred to a 100-mm dish coated with anti-Thy1.1 antibody (from hybridoma T11D7; American Type Culture Collection, Rockville, MD) for 45 min. Cells were then trypsinized off (1250 units/mL) (Sigma–Aldrich, St. Louis, MO) the petri dish and plated on coverslips coated with mouse-laminin (Trevigen Inc., Gaithersburg, MD). Cells were then cultured in a serum free defined media, DMEM (Invitrogen, Grand Island, NY) containing BDNF (50 ng/mL) (Peprotech, Rocky Hill, NJ), CNTF (10 ng/mL) (Peprotech, Rocky Hill, NJ), and forskolin (5 ng/mL) (Sigma–Aldrich, St. Louis, MO). Cells were incubated at 37 °C in a humidified atmosphere of 10% CO_2 and 90% air.

2.2. Intracellular calcium ($[Ca^{2+}]_i$) measurement

Purified RGCs were allowed to incubate in culture for 10 Days *in vitro* (D.I.V) before subjecting them to calcium imaging experiments. Intracellular calcium in purified RGCs was measured at 37 °C by the ratiometric technique using fura-2-AM (excitation at 340 nm and 380 nm, emission at 510 nm) (Invitrogen, Carlsbad, CA) as described by Prasanna et al. (2000) utilizing Nikon Eclipse TE2000-5 microscope and NIS-Elements AR3.2 software (Nikon Instruments, Melville, NY). The Grynkiewicz equation was used to convert the 340/380 ratio to internal levels of calcium in nanomolar (nM) concentrations (Grynkiewicz et al., 1985) using the kd value of 224 nM. During the calcium imaging studies, some cells were pretreated with (+)-SKF10047 (Tocris, Ellisville, MO), (+)-Pentazocine (Sigma–Aldrich, St. Louis, MO), BD1047 (Tocris, Ellisville, MO), or Verapamil (Tocris, Ellisville, MO) for 30 min before they were stimulated with potassium chloride (KCl). Peak calcium levels were calculated after KCl administration. Basal levels of cytoplasmic calcium were calculated 30 s prior to the administration of KCl. Peak cytoplasmic calcium levels were calculated after the administration of KCl.

2.3. Immunocytochemistry

Purified retinal ganglion cells were grown on coverslips and fixed with 100% methanol at −20 °C for 10 min or incubated at room temperature with paraformaldehyde for 15 min. These cells were then blocked with 5% normal donkey serum for 2 h at room temperature. Blocking solution was removed and cells were then incubated with primary antibodies: affinity-purified σ-1r monoclonal antibody (1/50 dilution; Santa Cruz Biotechnology, Santa Cruz, CA), voltage-dependent L-type-1C subunit antibody (1/100; Millipore, Temecula, CA), or *Thy1.1* monoclonal antibody (1/100 dilution; Santa Cruz Biotechnology, Santa Cruz, CA) at 4 °C overnight. Coverslips were then washed three times with PBS, and a 1:1000 dilution of secondary antibodies donkey anti-rabbit IgG (Alexa Fluor 648) conjugate and donkey anti-mouse IgG (Alexa Fluor 488) conjugate (Invitrogen, Carlsbad, CA) were added and incubated for 1 h in the dark. After incubation, the coverslips were washed again three times with PBS. Mounting was performed on glass slides using antifade reagent with DAPI (Prolong Gold; Invitrogen, Carlsbad, CA) and allowed to dry for 20 min in the dark. Cells were viewed on a confocal laser scanning microscope (LSM 510; Zeiss, Thornwood, NY).

2.4. Co-localization with immunofluorescence staining

Confocal microscopy was performed using a Zeiss LSM 510 META laser-scanning microscope (Carl Zeiss, Inc., Thornwood, NY) equipped with a 40× objective, using the following laser wavelengths: excitation 488 nm, emission 505–530 nm or excitation 648 nm, emission 630–700 nm. Quantifications of the co-localization coefficients, derived from measured pixel overlaps between sigma-1

receptor and L-type Voltage Gated Calcium Channels, were performed using a free, open source software package, BioImageXD (Kankaanpää et al., 2006). To quantify the level of co-localization, 9 cells were randomly selected from 3 separate experiments and optically sectioned using confocal microscope. At least 15 z-slices at 0.25 μm thickness were obtained per cell. Co-localization was evaluated from the center slice of the cell by examination of the merged images and analysis was performed with BioImageXD. The co-localization thresholds were calculated automatically by the BioImageXD software, as recommended by Costes et al. (2004). As described by Manders et al., 1993, co-localization coefficient 1 (M1/tM1) and co-localization coefficient 2 (M2/tM2) were used to identify the proportion of overlap between one protein on another. Utilizing Manders coefficients calculations enable co-localization coefficients to be calculated independent of the relative intensities of the two different channels (Manders et al., 1993). A pseudo color of yellow was utilized to depict co-localization of sigma-1 receptor with the L-VGCC.

2.5. Western blot analysis

Primary neurons were homogenized in 100 μL of ice cold buffer containing 50 mM Tris, pH 7.4, 10 mM Mg^{2+}, 1 mM EDTA, 1 mM EGTA, 10 mM benzamide, 100 ng/mL leupeptin, 100 ng/mL aproteinin, 0.08 mM sodium molybdate, 0.01% triton-100, 10 μM okadoic acid, and 2 mM sodium pyrophosphate. Lysed aliquots were sonicated and taken for protein concentration estimation using protein assay reagent (Bio-Rad Laboratories, Hercules, CA). Samples were then electrophoresed on a pre-cast ready-made SDS/PAGE gradient gel (Bio-Rad Laboratories, Hercules, CA). The protein was then transferred onto a PVDF membrane (Millipore, Billerica, MA) overnight at 4 °C. Membranes were then blocked for 1 h with 4% non-fat dried milk (Bio-Rad Laboratories, Hercules, CA), and then probed overnight at 4 °C. A mouse monoclonal antibody against sigma-1 receptor (Santa Cruz Biotechnology, Santa Cruz, CA) was used at a 1:1000 dilution. A polyclonal antibody against voltage-dependent L-type-1C subunit antibody (Millipore, Temecula, CA) was used at a 1:1000 dilution. Membranes were then incubated at room temperature for 1 h with a horseradish peroxidase conjugated secondary antibody (Bio-Rad Laboratories, Hercules, CA) at a dilution of 1:1000. The proteins were then visualized with supersignal chemiluminesence (Pierce Biotechnology, Rockford, IL) using UVP software (Upland, CA).

2.6. Total Internal Reflection Fluorescence Microscopy (TIFRM)

TIRFM was used to obtain images of the cell membrane from a distance of 100 nm from the coverslip to be thin enough to allow only the plasma membrane to get illuminated. The Olympus IX71 fluorescence microscope (Olympus America Inc., Melville, NY) was used to measure single cell evanescent field fluorescence (EFF) intensity using an Olympus 60×/1.45 Oil objective. Cells were excited with 488 nm with an argon air-cooled laser (Melles Griot, Albuquerque, New Mexico). Fluorescence images were collected with a back-illuminated electron-multiplying charge-coupled device (EMCCD) camera (Hamamatsu Photonics, Japan). Simple PCI software was used to control the protocol of acquisition and to perform data analysis.

2.7. Data analysis

Statistical significance of differences between values was evaluated by performing one-tailed unpaired *t*-test for two group comparisons and ANOVA followed by Student-Newman–Keuls post hoc test for multiple group comparisons. Experimental data with values of $p < 0.05$ were considered to be statistically significant.

3. Results

3.1. Purified rat retinal ganglion cell culture

Retinas were isolated from P3 to P7 Sprague Dawley rat pups. Utilizing a double immunopanning technique described by Barres et al. (1988), microglia were eliminated from the mixed culture by panning with an anti-macrophage antibody. RGCs were then collected from the retinal cell population by panning with a T11D7 (anti-thy1.1) antibody. Cells were allowed to mature for 10 days before subjecting them to immunocytochemistry analysis. Fig. 1A and B, demonstrate that the majority of DAPI stained RGCs are thy1.1 positive. Fig. 1C and D demonstrate negative controls and in 1D where immunostaining was performed with the exclusion of the primary antibody.

3.2. Expression of sigma-1 receptor and L-type VGCCs in purified RGCs in culture

To determine whether σ-1 receptor and L-type VGCC were expressed in our purified primary RGCs, we examined extracts from purified P10 RGCs by Western blot analysis. σ-1 receptor and L-type VGCC were detected in RGC extracts after 10 days in culture (Fig. 2).

3.3. Plasma membrane staining (TIRFM) of sigma-1 receptor and co-localization of sigma-1 receptor and L-type Voltage Gated Calcium Channel in purified retinal ganglion cells

To determine the localization of σ-1 receptors and L-type VGCCs, we performed immunostaining on RGCs after 10 days in culture using a σ-1 receptor and L-type VGCC specific antibodies. Total Internal Reflection Fluorescence Microscopy (TIRFM) revealed that immunoreactivity for σ-1 receptors was distributed throughout the plasma membrane of the soma and proximal neurites of our purified RGCs (Fig. 3B). Bright field microscopy images were obtained of the purified RGCs (Fig. 3A). Confocal immunocytochemistry was performed looking at the L-type VGCC and the σ-1r (Fig. 3C–F). As described in Section 2.4, Z-stack sections of 0.25 μm thickness were taken on the Zeiss 510 confocal and the extenet of pixel overlap in the merged images was calculated using the BioImageXD software. Co-localization calculations confirm in purified RGCs that about 50% of the L-type VGCCs are co-localized with σ-1rs and that 67% of the σ-1rs are co-localized with L-type VGCCs (Fig. 3F, depicted as yellow, and 3G). This data suggests that the L-type VGCC and the σ-1r are co-compartmentalized in similar cellular locations in purified RGCs.

3.4. KCl-induced calcium influx in purified RGCs is mediated through L-type VGCCs in an extracellular calcium dependent manner

We initiated a set of Ca^{2+} imaging experiments to assess the fraction of the KCl-activated Ca^{2+} concentration change on purified RGCs (Fig. 4A and B). In addition, purified RGCs were incubated in Verapamil (10 μM) (a known L-type VGCC blocker) for 30 min prior to KCl stimulation to assess the percentage of L-type VGCCs that were activated by KCl stimulation (Fig. 4A and B). Before the stimulation of KCl, the average baseline $[Ca^{2+}]_i$ levels were equal to 149 ± 8 nM ($n = 110$) and 154 ± 16 nM ($n = 31$) for control KCl stimulated cells and for Verapamil (10 μM) treated cells. Treatment with KCl to elicit purified RGC depolarization robustly increased cytoplasmic calcium in purified RGCs to 1942 ± 118 nM ($n = 110$)

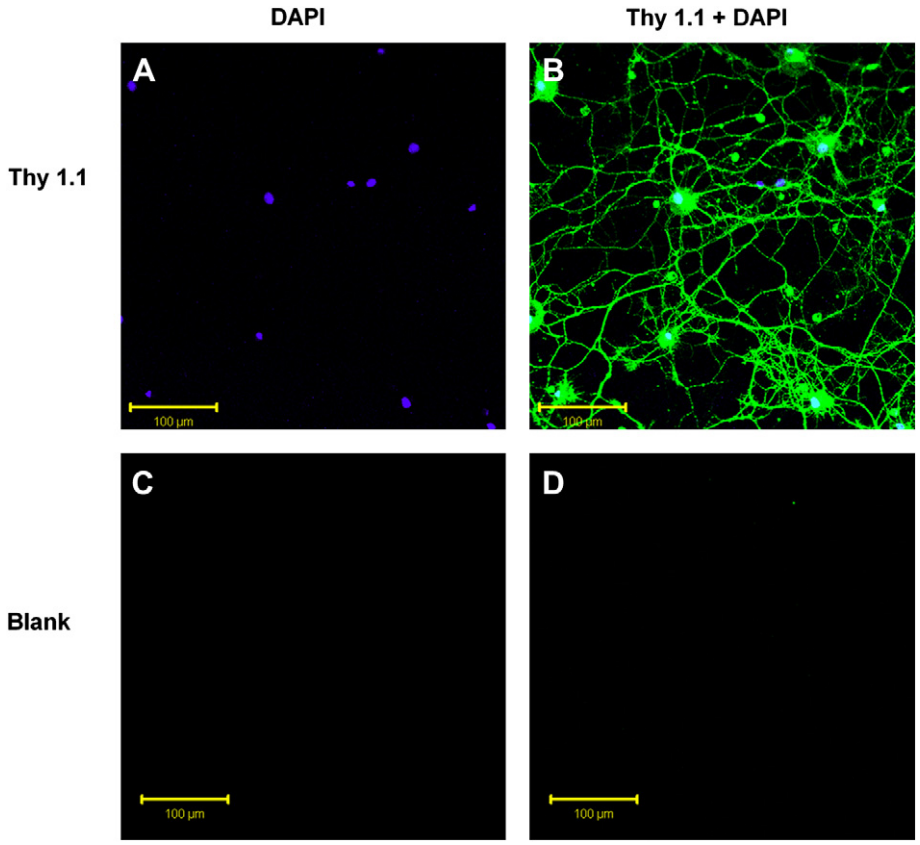

Fig. 1. Characterization of isolated RGCs utilizing a double immunopanning procedure described by Barres et al. (1988). Purity of RGCs was assessed through immunocytochemical analysis of RGC specific markers of Thy-1.1. Thy1.1 was detected in almost all DAPI stained cells in our purified cultures. Top panel represents staining with specific primary antibody (**A**) nuclei stained with DAPI (blue). (**B**) Immunolabeling of primary RGCs with an antibody against Thy-1.1 (Green); nuclei stained with DAPI (blue). Bottom panel represents the negative control in which immunostaining was performed with the exclusion of the primary antibody. (**C**) Blank. (**D**) Donkey anti-Rabbit alexa 488 alone. Scale bar, 100 µm.

(Fig. 4A and B); while Verapamil pre-treated cells decreased the KCl calcium stimulation to 838 ± 81 nM ($n = 31$). These results suggest that KCl stimulation in purified RGCs mediates 57% of the calcium ion influx through L-type VGCCs and 43% of the calcium ion influx through non-L-type VGCCs. To determine that extracellular calcium was required for KCl-induced calcium signaling, extracellular calcium was removed from the buffer, and there was no KCl stimulated calcium influx until 2.5 mM of $CaCl_2$ was administered to the extracellular calcium buffer solution (Fig. 4C).

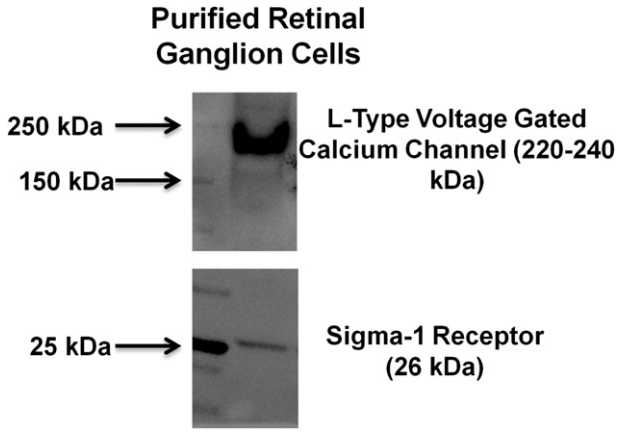

Fig. 2. Purified RGCs express σ-1r and L-type VGCC *in vitro*. Immunoblots performed on cellular lysates from P3-P7 RGCs after 10 days in culture show the expression of σ-1r and L-type VGCCs.

3.5. SKF-10047 (Sigma-1 receptor agonist) decreases peak calcium ion influx through VGCCs in a dose dependent manner while antagonizing sigma-1 receptor potentiates peak calcium ion influx through VGCCs

It has been reported previously in a non-retinal ganglion cell line that (+)-SKF10047 (σ-1 receptor agonist) decreased calcium ion influx following KCl stimulation (Tchedre et al., 2008). To determine if (+)-SKF10047 had a concentration dependent effect on the attenuation of KCl induced calcium ion influx in purified RGCs, calcium imaging was performed with fura-2-AM Ca^{2+} imaging dye following treatment with different doses of (+)-SKF10047. Purified RGCs were pre-incubated with 100 nM, 1 µM, and 10 µM of (+)-SKF10047 for 30 min prior to KCl stimulation (Fig. 5A–C). Average baseline $[Ca^{2+}]_i$ levels were equal to 149 nM ± 8 ($n = 110$), 148 nM ± 12 ($n = 53$), 110 nM ± 12 ($n = 37$), and 101 nM ± 15 ($n = 42$) for untreated control cells, and cells treated with 100 nM, 1 µM, and 10 µM of (+)-SKF10047 respectively (Fig. 5B). Peak KCl induced $[Ca^{2+}]_i$ levels were equal to 1942 nM ± 118 ($n = 110$), 1835 nM ± 150 ($n = 53$), 1271 nM ± 138 ($n = 37$), and 1382 nM ± 150 ($n = 42$) for untreated control cells, and cells treated with 100 nM, 1 µM, and 10 µM of (+)-SKF10047 respectively (Fig. 5A).

To determine the contribution of endogenous σ-1 receptor to the calcium signaling response, purified RGCs were first pre-incubated with 100 nM, 1 µM, and 10 µM of BD1047 (σ-1 antagonist) for 30 min prior to KCl stimulation (Fig. 5D and E). For the σ-1 receptor antagonist treated cells (BD1047) average baseline $[Ca^{2+}]_i$ levels were equal to 149 nM ± 8 ($n = 110$), 168 nM ± 21 ($n = 52$),

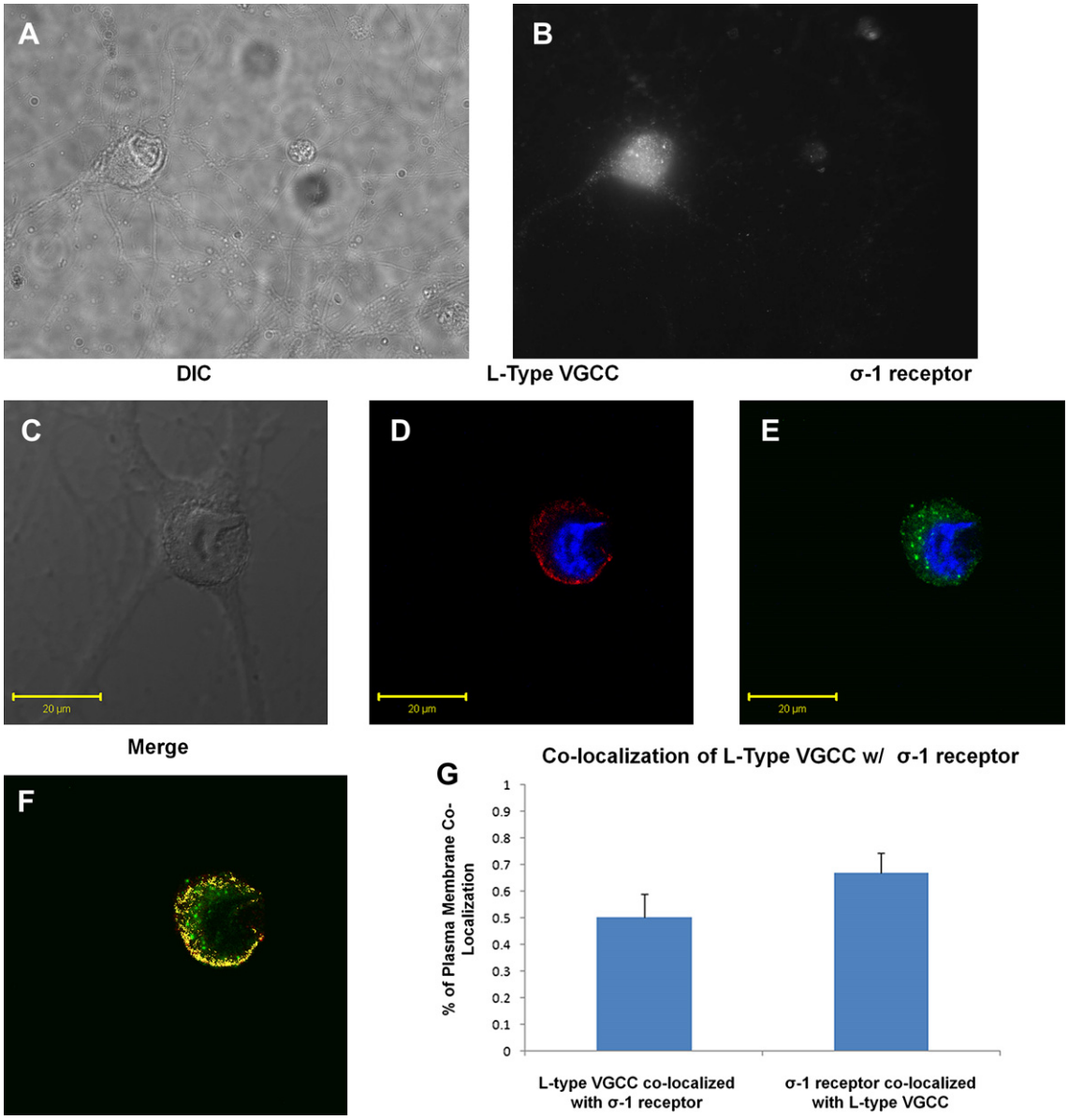

Fig. 3. TIRFM indicating plasma membrane localization of σ-1 and immunocytochemical colocalization of σ-1 receptor and L-type VGCCs in purified RGCs. (**A**) Bright Field Microscopy image of purified RGCs used for TIRFM analysis. (**B**) TIRFM image of purified RGCs demonstrating σ-1 expression on the plasma membrane of primary RGCs. (**C**) DIC image of RGC; (**D**) L-type Voltage Gated Calcium Channel (VGCC) expression (Red) and DAPI (Blue) and (**E**) σ-1 receptor expression (Green) and DAPI (Blue). Z-stack images were obtained at 0.25 μm intervals in a Zeiss 510 confocal microscopy for **D**, **E** and **F**. Bars, 20 μm. (**F**) Merged pictures of **D** and **E**, demonstrated co-localization of the two proteins (co-localizing voxels are presented as yellow). Bars, 20 μm. (**G**) Co-localization calculations demonstrate that 50% of L-type VGCCs are co-localized with σ-1 receptors, and that 67% of σ-1 receptors are co-localized with L-type VGCCs.

172 nM ± 21 (n = 34), and 303 nM ± 21 (n = 61) for untreated control cells, and cells treated with 100 nM, 1 μM, and 10 μM of BD1047 respectively. For peak KCl induced $[Ca^{2+}]_i$ levels were equal to 1942 nM ± 118 (n = 110), 1707 nM ± 190 (n = 52), 2650 nM ± 344 (n = 34), and 1898 nM ± 154 (n = 61) for untreated control cells, and cells treated with 100 nM, 1 μM, and 10 μM of BD1047 respectively (Fig. 5D and E).

These results suggested that (+)-SKF10047 (100 nM, 1 μM, and 10 μM) was able to significantly inhibit baseline levels of cytoplasmic calcium and KCl-induced calcium signaling in a dose dependent manner ($p < 0.05$) (Fig. 5A–C). These results also suggested that the σ-1r antagonist BD1047 potentiated KCl-induced calcium signaling at 1 μM ($p < 0.01$) (Fig. 5D and E). Additionally at 10 μM treatment, BD1047 significantly increased the baseline level of cytoplasmic calcium by 2 fold ($p < 0.001$), but had no effect on peak level of KCl-induced calcium signaling (Fig. 5E).

3.6. Sigma-1 receptor agonists decreased KCl-Induced calcium ion influx in purified RGCs which is reversed by a Sigma-1 receptor antagonist treatment

Pentazocine was also tested to investigate if another σ-1 receptor agonist pretreatment 30 min before KCl stimulation could decrease calcium ion influx through KCl stimulated VGCCs in purified RGCs. Average baseline $[Ca^{2+}]_i$ levels were equal to 149 nM ± 8 (n = 110), 110 nM ± 12 (n = 37), and 186 nM ± 15 (n = 53) for untreated control cells, and cells treated with (+)-SKF10047 (1 μM) or Pentazocine (1 μM). Peak KCl induced

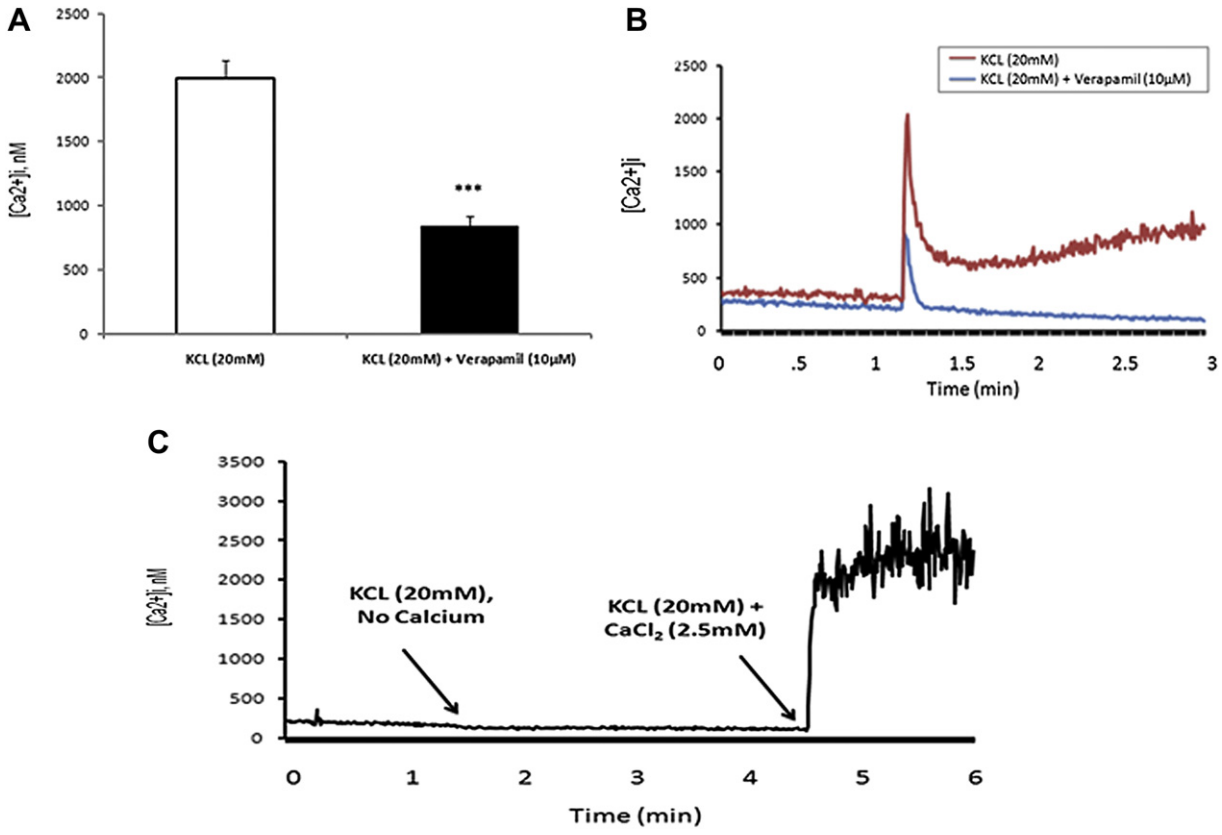

Fig. 4. KCl depolarization produced an increase in cytoplasmic calcium response through VGCCs in an extracellular calcium dependent manner. KCl-induced calcium influx was measured by fura-2-AM imaging. Cells were preincubated for 30 min with either fura-2-AM or fura-2-AM and Verapamil (10 μM) before stimulating the cells with 20 mM KCL. (**A**) Verapamil significantly inhibited KCl-induced calcium influx in purified RGCs. Values are mean ± SEM (n = 110 for KCl; n = 31 for Verapamil + KCl) (***$p < 0.001$). (**B**) Representative $[Ca^{2+}]_i$ trends in response to KCl and KCl + Verapamil (10 μM). (**C**) Representative tracing depicting the effect of extracellular calcium on KCl-induced calcium signaling. Purified RGCs were preincubated with fura-2-AM in a calcium-free buffer for 30 min before stimulation with KCl in the absence and presence of calcium (2.5 mM).

$[Ca^{2+}]_i$ levels were found to be 1942 nM ± 118 (n = 110), 1271 nM ± 138 (n = 37), and 1412 nM ± 77 (n = 53) for untreated control cells, and cells treated with (+)-SKF10047 (1 μM) or Pentazocine (1 μM) (Fig. 6A and B).

To determine if the suppression of KCl-induced calcium ion influx with the two σ-1 receptor agonists was being mediated through the σ-1 receptor, calcium imaging experiments were performed with the co-application of BD1047 (σ-1 receptor antagonist) either with SKF10047 or Pentazocine (Fig. 6C and D). Purified RGCs were treated with BD1047 5 min prior to the administration of the two σ-1 receptor agonists. Cells were then incubated for 30 min with both agonist and antagonist before KCl stimulation. Average baseline $[Ca^{2+}]_i$ levels were equal to 118 nM ± 8 (n = 43), 85 nM ± 8 (n = 34), and 82 nM ± 15 (n = 31) for untreated control cells, and cells treated with a combination of either BD1047 (10 μM) and (+)-SKF10047 (1 μM), or cells treated with BD1047 (10 μM) and Pentazocine (1 μM) respectively. Peak KCl induced $[Ca^{2+}]_i$ levels were equal to 800 nM ± 70 (n = 43), 700 nM ± 101 (n = 34), and 753 nM ± 90 (n = 31) for untreated control cells, and cells treated with a combination of either BD1047 (10 μM) and (+)-SKF10047 at 1 μM, or with BD1047 (10 μM) and Pentazocine (1 μM) respectively (Fig. 6C and D).

(+)-SKF10047 (1 μM) and pentazocine (1 μM), significantly suppressed the peak KCl-induced calcium ion influx by 35% ($p < 0.01$) and 27% ($p < 0.01$) respectively (Fig. 6A and B). Additionally, the co-administration of a σ-1 receptor agonist with a σ-1 receptor antagonist blocked the σ-1 agonist induced suppression of peak KCl-induced calcium ion influx (Fig. 6C and D). These results suggested that the blockade effect observed by both (+)-SKF10047 and pentazocine were mediated through the σ-1 receptor and not some other non-specific ligand binding site. The results are in agreement with Hayashi et al. (2000) that found in NG108 cells that σ-1r agonist effects on activated VGCCs were able to be abolished through the co-application of an antisense oligodeoxynucleotide targeted against σ-1r, and Tchedre et al. (2008) who also demonstrated in a non-retinal ganglion cell line that σ-1r agonist effects on activated VGCCs were acting via the σ-1r through the ability to block the agonist mediated effects by the co-treatment of a σ-1r antagonist.

3.7. Sigma-1 receptor mediated effects on KCl induced calcium ion influx were mediated through the L-type voltage gated calcium channel

Studies have suggested that there is a direct interaction between σ-1 and L-type VGCCs (Tchedre et al., 2008). We wanted to determine if the observed σ-1 receptor ligand effects on KCl induced calcium ion influx were being mediated through the L-type VGCCs or other VGCCs in purified RGCs. To address this issue, purified RGCs were co-treated with a σ-1 receptor ligand (SKF-10047, Pentazocine, or BD1047) and Verapamil (L-type VGCC blocker). Cells were first treated with Verapamil (10 μM) 5 min before the administration of a σ-1 receptor ligand. These cells were then incubated for 30 min with both Verapamil and σ-1 receptor ligand prior to KCl stimulation. Average baseline $[Ca^{2+}]_i$ levels were equal to 118 nM ± 8 (n = 43), 80 nM ± 9 (n = 44), 113 nM ± 12 (n = 41),

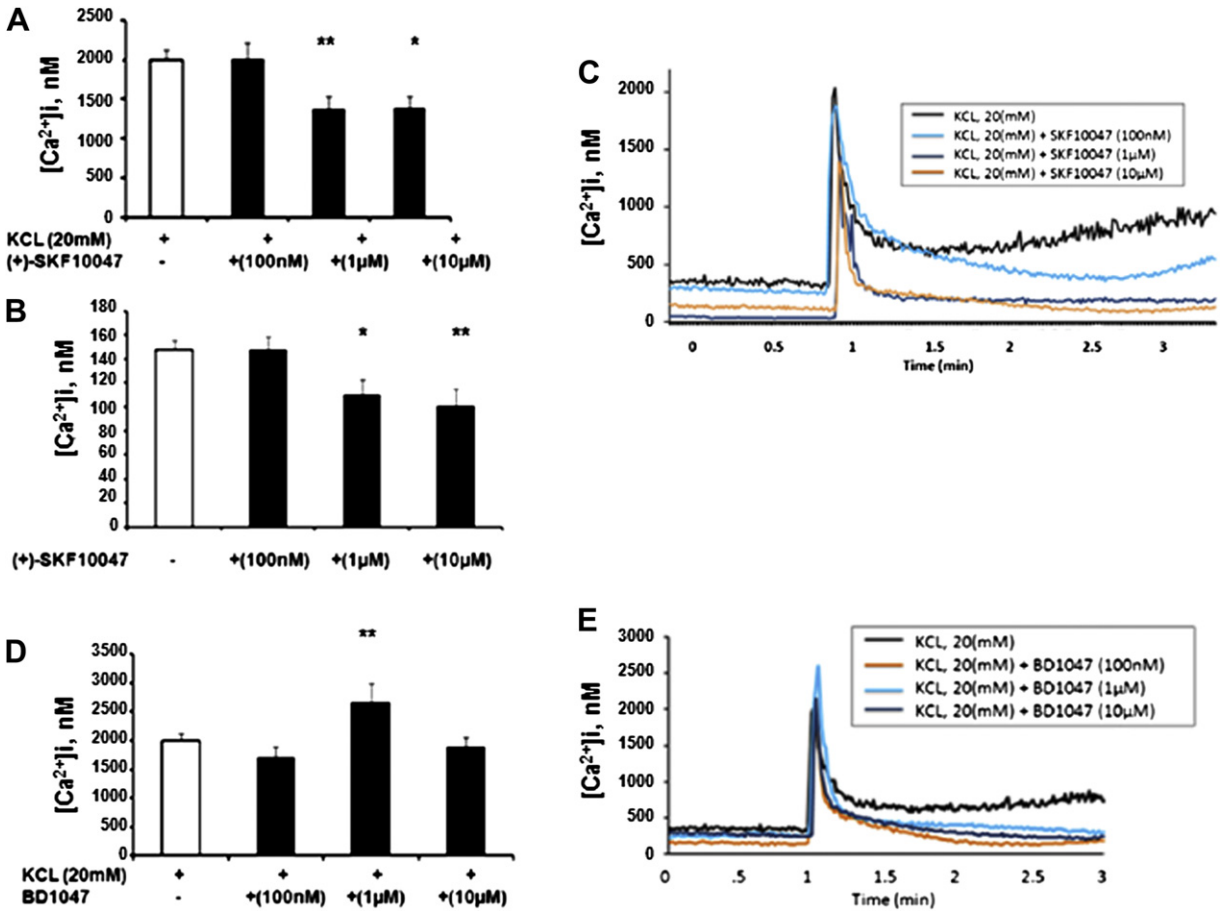

Fig. 5. The effect of sigma-1 receptor agonist, (+)-SKF10047, and antagonist on basal level of cytoplasmic calcium and KCl-induced calcium influx in purified RGCs. KCl-induced calcium influx was measured by fura-2-AM imaging. Cells were incubated with fura-2-AM with and without (+)-SKF10047 for 30 min before stimulating the cells with KCl. After treatment, all drugs remained in the bath solution for the duration of the calcium imaging experiments. (**A**) Sigma-1 agonist, (+)-SKF10047, inhibited KCl-induced calcium influx in a concentration-dependent manner. Values are represented as mean ± SEM ($n = 110$ for KCl; $n = 53$ for KCl + (+)-SKF10047 (100 nM); $n = 37$ for KCl + (+)-SKF10047 (1 μM); $n = 42$ for KCl + (+)-SKF10047 (10 μM)) (** = $p < 0.01$ and * = $p < 0.05$). (**B**) Summary of the effects that (+)-SKF10047 has on basal level of cytoplasmic calcium. Values are mean ± SEM ($n = 110$ for KCl; $n = 53$ for KCl + (+)-SKF10047 (100 nM); $n = 37$ for KCl + (+)-SKF10047 (1 μM); $n = 42$ for KCl + (+)-SKF10047 (10 μM)) (**$p < 0.01$ and *$p < 0.05$). (**C**) Representative tracing depicting the effect of various concentrations of (+)-SKF10047 on KCl induced peak $[Ca^{2+}]_i$. (**D**) Sigma-1 antagonist, BD1047 (1 μM), demonstrated a statistical significant potentiation of KCl-induced calcium influx. Values are represented as mean ± SEM ($n = 110$ for KCl; $n = 52$ for KCl + BD1047 (100 nM); $n = 34$ for KCl + BD1047 (1 μM); $n = 61$ for KCl + BD1047 (10 μM)) (**$p < 0.01$). (**E**) Representative graph depicting the effect of various concentrations of BD1047 on KCl induced peak $[Ca^{2+}]_i$.

91 nM ± 7 ($n = 43$), and 117 nM ± 12 ($n = 42$) for untreated control cells, or cells treated with Verapamil (10 μM), or with a combination of either Verapamil (10 μM) and BD1047 (1 μM), or Verapamil (10 μM) and (+)-SKF10047 (1 μM), or Verapamil (10 μM) and (+)-pentazocine (1 μM) respectively. Peak KCl induced $[Ca^{2+}]_i$ levels were equal to 800 nM ± 70 ($n = 43$), 342 nM ± 56 ($n = 44$), 286 nM ± 35 ($n = 41$), 332 nM ± 41 ($n = 43$), and 234 nM ± 36 ($n = 42$) for untreated control cells, or cells treated with Verapamil (10 μM), or with a combination of either Verapamil (10 μM) and BD1047 (1 μM), or Verapamil (10 μM) and (+)-SKF10047 (1 μM), or Verapamil (10 μM) and (+)-pentazocine (1 μM) respectively (Fig. 7A and B). The control untreated cells had a statistically significant increase in KCl induced $[Ca^{2+}]_i$ compared to all other treated cells, $p < 0.001$ (Fig. 7A and B). However, there was no difference in KCl induced $[Ca^{2+}]_i$ amongst all the treated cells. These results suggest that the σ-1 receptor ligand mediated effects in Figs. 4–6 were all acting through σ-1 receptor to modulate the L-type VGCCs.

These results suggest, for the first time in primary RCGs, that σ-1 receptor stimulation (Fig. 8) regulates $[Ca^{2+}]_i$ influx through L-type VGCCs (Fig. 8B). Also, the antagonizing of σ-1 receptor appears to increase $[Ca^{2+}]_i$ influx through L-type VGCCs (Fig. 8C). This implies that perhaps σ-1 receptor has a homeostatic regulatory role in the regulation of L-type VGCCs which is independent of ligand binding (Fig. 8A).

4. Discussion

Two σ-1r agonists (SKF10047 and (+)-pentazocine) decreased calcium ion influx through KCl stimulated VGCCs, while co-treatment with a σ-1r antagonist (BD1047) abolished the inhibitory effect of the two σ-1r agonists, suggesting that the agonist effects were mediated through σ-1rs. The co-treatment of a known L-type VGCC blocker (Verapamil) with the two σ-1r agonists resulted in no further decrease in calcium ion influx through the activated VGCCs when compared to RGCs treated with verapamil alone. Taken together, our study suggests that σ-1r receptor stimulation attenuates calcium influx through L-type VGCCs and this is being reported for the first time in purified RGCs.

The data supports previous observations in other tissues that σ-1r ligands impede calcium ion influx through activated VGCCs. However, our results in purified RGCs differ from previous studies in other cell types, by specifically identifying L-type VGCCs and not other sub-types of VGCCs, as the main target of σ-1r activation. Other studies also demonstrate that σ-1r ligands act independent of σ-1r to block VGCCs. Research in hippocampal neurons (Church

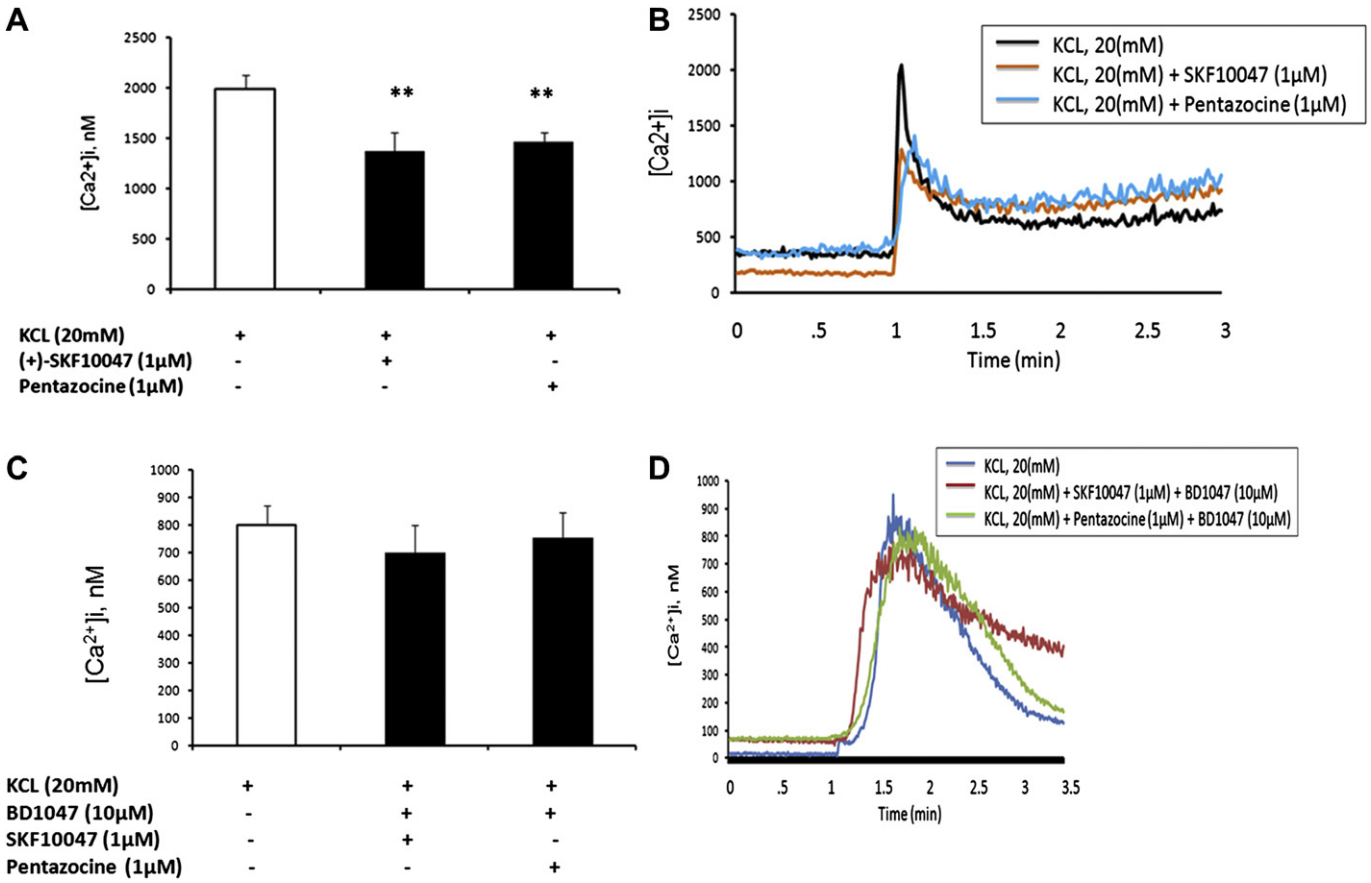

Fig. 6. Effect of sigma-1 receptor ligand (+)-SKF10047 (1 μM) and pentazocine (1 μM) on KCl-induced (20 mM) peak calcium influx in primary RGCs. KCl-induced calcium influx was measured by fura-2-AM imaging. In calcium imaging studies, cells were preincubated for 30 min with fura-2-AM alone, fura-2-AM + (+)-SKF10047, or fura-2-AM + pentazocine. (**A**) Sigma receptor agonists ((+)-SKF10047 and pentazocine) inhibited KCl-induced peak calcium influx in primary RGCs. Values are mean ± SEM ($n = 110$ for KCl; $n = 37$ for KCl + (+)-SKF10047; $n = 53$ for KCl + pentazocine) (**$p < 0.01$). (**B**) Representative tracing depicting the effect of (+)-SKF10047 or pentazocine on KCl induced peak $[Ca^{2+}]_i$. (**C**) Co-treatment of a sigma-1 receptor antagonist abolished the inhibitor effects of (+)-SKF10047 and pentazocine on KCl-induced peak calcium influx in primary RGCs. Values are mean ± SEM ($n = 43$ for KCl; $n = 34$ for KCl + (+)-SKF10047 (1 μM) + BD1047 (1 μM); and $n = 31$ for KCl + pentazocine (1 μM) + BD1047 (1 μM)). (**D**) Representative tracing depicting the effect of BD1047 treatment on (+)-SKF10047 or pentazocine on KCl induced peak $[Ca^{2+}]_i$.

and Fletcher, 1995) and parasympathetic and sympathetic neurons (Zhang and Cuevas, 2002) demonstrated that σ-1r ligands, both agonist (pentazocine) and antagonist (haloperidol), at high micromolar concentrations decreased calcium ion influx through all VGCCs in a σ-1r independent manner. Similarly, a study performed using mouse forebrain synaptosomes demonstrated that σ-1r ligand treatment at high micromolar concentrations (agonist (pentazocine) and antagonist (BD10047)) decreased calcium ion influx through non-L type VGCCs in a σ-1r independent manner (González et al., 2012).

An explanation for the difference in these results could be the differing response of various neuronal cell types and doses of σ-1r ligands used to treat these neuronal cultures in each of these experimental paradigms. Blockade of VGCCs by pentazocine (σ-1r agonist) was observed only at doses ≥ 100 μM in the studies performed in primary hippocampal neurons and parasympathetic and sympathetic neurons (Zhang and Cuevas, 2002; Church and Fletcher, 1995). It is unclear if these two studies could demonstrate blockade of VGCCs with pentazocine at lower micromolar or nanomolar concentrations because they did not report any data at those lower pharmacological concentrations (Zhang and Cuevas, 2002; Church and Fletcher, 1995). González et al. (2012) reported that in the mouse forebrain synaptosomes that they were unable to block stimulated VGCCs with pentazocine at concentrations at 10 μM. Our results are in agreement with this finding since the mouse forebrain synaptosomes do not have L-type VGCCs (Alvarez et al., 1995; Meder et al., 1997).

The studies described above used high micromolar concentrations of σ-1r ligands and this may result in binding to other receptors that could produce confounding effects on VGCCs. For instance, haloperidol is a very well-studied σ-1r antagonist; however, it has been demonstrated to have strong antiadrenergic, antihistaminic, and anti-serotonin activity. Pentazocine, widely used as a σ-1r agonist, has partial agonistic like effects on μ and κ opioid receptors. Therefore, when high micromolar concentrations of σ-1r ligands are used, it is difficult to clearly identify the mechanism associated with actions on the VGCCs.

Our findings concur with those from other studies demonstrating the ability of σ-1r ligands to modulate calcium ion influx through activated VGCCs in a σ-1 receptor dependent manner (Hayashi et al., 2000; Tchedre et al., 2008; Tchedre and Yorio, 2008). Since we demonstrated that the σ-1r agonist-like effects on VGCCs were reversed by a co-application of BD1047 (σ-1r antagonist), it appears that σ-1r has a functional relationship on the attenuation of VGCCs, and specifically the L-type VGCCs, in purified RGCs.

Another interesting point in our study was that BD1047 (σ-1r antagonist) produced an increased response to KCl induced calcium signaling in RGCs (Fig. 5). This is in agreement with a previous study that demonstrated that BD1047 had an opposite effect compared to a σ-1r agonist on intracellular calcium mobilization (Novakova

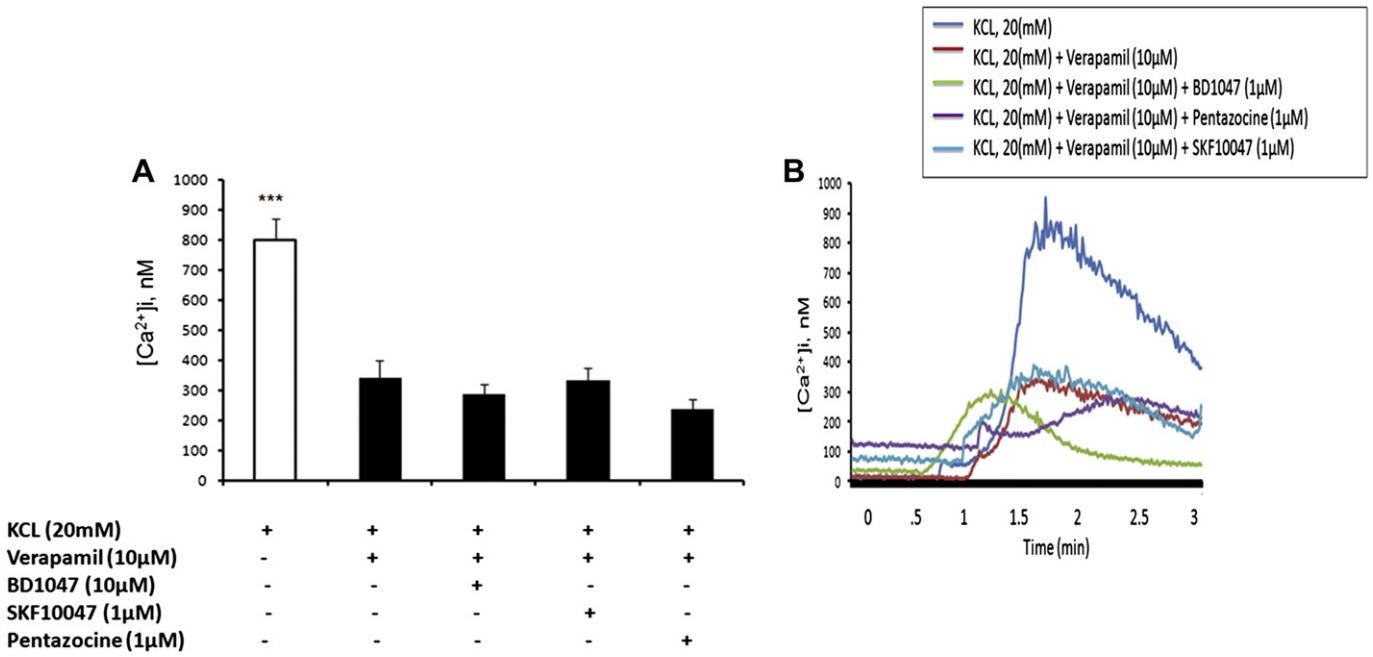

Fig. 7. Effect of sigma-1 receptor ligands (1 μM) co-treated with the L-type VGCC blocker Verapamil (10 μM) on KCl-induced (20 mM) peak calcium influx in purified RGCs. KCl-induced calcium influx was measured by fura-2-AM imaging. In calcium imaging studies, cells were preincubated for 30 min with fura-2-AM alone, fura-2-AM + Verapamil (10 μM), fura-2-AM + Verapamil + BD1047, fura-2-AM + Verapamil + (+)-SKF10047, or fura-2-AM + Verapamil + pentazocine. (**A**) Verapamil inhibited KCl-induced peak calcium influx in primary RGCs by 57%. There was no appreciable difference in KCl-induced peak calcium influx for cells treated with Verapamil and cells treated with Verapamil and sigma-1 receptor ligands. Values are mean ± SEM ($n = 43$ for KCl treated cells; $n = 44$ for KCl + Verapamil (10 μM); $n = 41$ for KCl + Verapamil (10 μM) + BD1047 (1 μM); $n = 43$ for KCl + Verapamil + (+)-SKF10047; and $n = 42$ for KCl + Verapamil + Pentazocine) (***$p < 0.001$). (**B**) Representative tracing depicting the effect Verapamil (10 μM), Verapamil (10 μM) + BD1047 (1 μM), Verapamil (10 μM) + (+)-SKF10047, or Verapamil (10 μM) + pentazocine on KCl induced peak $[Ca^{2+}]_i$.

et al., 1998). Several reports have also demonstrated that σ-1r can alter channel functions in the absence of a ligand implying that this receptor has baseline effects (Aydar et al., 2002; Tchedre and Yorio, 2008). Our results suggest that BD1047 diminished the homeostatic regulation of σ-1r on L-type VGCCs, and subsequently caused an increase of calcium signaling likely through the L-type VGCC.

This potentiation effect of BD1047 was observed at 1 μM concentrations but was non-existent at 10 μM concentrations. These anomalous pharmacological effects can be explained by another study that demonstrated that a 10 μM treatment of BD-1047 decreased KCl induced calcium ion influx in non-L-type VGCCs in mouse forebrain synaptosomes isolated from σ-1r

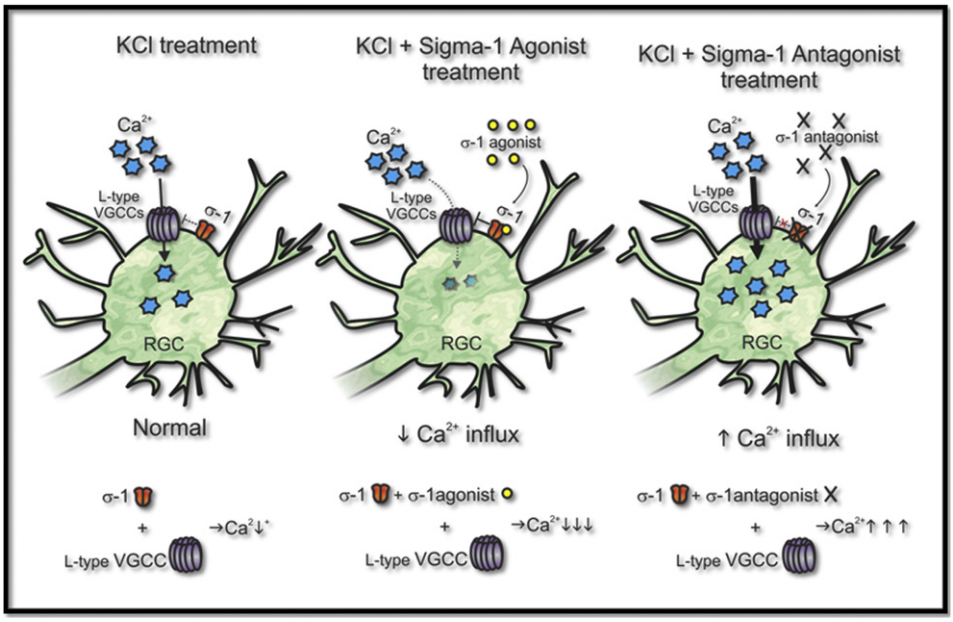

Fig. 8. Sigma-1r appears to have a homeostatic role in regulating calcium ion influx through RGCs. (**A**) Under normal conditions, σ-1r may have a role in attenuating $[Ca^{2+}]_i$ influx through L-type VGCCs. (**B**) Sigma-1 receptor agonist stimulation decreases $[Ca^{2+}]_i$ through L-type VGCCs. (**C**) When σ-1rs are antagonized, there is an increased level of $[Ca^{2+}]_i$ by influx through L-type VGCCs.

knockout mice (González et al., 2012). Therefore, it could be possible in purified RGCs that BD1047 at higher micromolar concentrations can be simultaneously potentiating calcium ion influx through L-type VGCCs while activating other mechanisms that could be diminishing calcium ion influx through other non-L-type VGCCs. In addition, there have been described sub-populations of retinal ganglion cells (REF) and this could result in heterogeneity of the response.

The detailed molecular signaling pathways responsible for σ-1r mediated regulation of different ion gated and voltage gated channels remains largely unknown. Studies have proposed that σ-1rs modulate intracellular signaling transduction through direct protein–protein interactions (Tchedre et al., 2008; Aydar et al., 2002; Lupardus et al., 2000). So far, σ-1r has been co-immunoprecipitated with L-type VGCCs (Tchedre et al., 2008) and potassium channels (Aydar et al., 2002; Lupardus et al., 2000). Our co-localization data in purified RGCs is in agreement with the above studies, and suggest that σ-1r is co-localized with L-type VGCCs in purified RGCs. In addition, Fig. 3 demonstrates through TIRF analysis that σ-1rs are present on neuronal plasma membrane of RGCs. This provides further evidence that in purified RGCs, σ-1r and L-type VGCCs are at the very least in close proximity to one another and have the potential to interact. However, some reports have also linked σ-1rs to the activation and modulation of G-protein coupled receptors (Zhang et al., 2011; Morin-Surun et al., 1999; Soriani et al., 1999; Ueda et al., 2001; Meyer et al., 2002). It is possible that this may be another mechanism that σ-1rs utilize to modulate calcium signaling through L-type VGCCs.

There have been numerous studies demonstrating neuroprotection of RGCs by blocking calcium ion influx through VGCCs. Intraperitoneal injections of nifedipine (L-type VGCC blocker) protected rats from ischemia-induced retinal degeneration damage (Crosson et al., 1990). Lomerizine, another L-type VGCC blocker, has been shown *in vitro* and *in vivo* studies to provide neuroprotection to retinal neurons when they were subjected to ischemic conditions (Toriu et al., 2000). Lastly, betaxolol, demonstrated neuroprotective like effects on RGCs. Betaxolol is commonly known as an intraocular pressure lowering agent, but was hypothesized to have its neuroprotective effects through its ability to block calcium ion influx through L-type VGCCs (Hirooka et al., 2000). Similar to the compounds above, it is possible that σ-1r activation can mediate its RGC neuroprotective effects through its ability to partially block calcium ion influx through activated L-type VGCCs.

In conclusion (Fig. 8), we demonstrate for the first time in purified RGCs that the activation of σ-1rs following agonist stimulation results in a suppression of calcium signaling through L-type VGCCs. We also demonstrate that antagonizing σ-1rs with an antagonist potentiates cytoplasmic calcium ion influx through L-type VGCCs. It is unclear if the σ-1r mediated effects on L-type VGCCs in primary RGCs are due to a direct protein–protein interaction, or some other secondary mechanism. Future studies are needed to investigate how this dynamic receptor interacts with L-type VGCCs in primary RGCs. The elucidation of this mechanism may help identify the endogenous function of this receptor, and may help explain how this receptor is neuroprotective.

Acknowledgments

This work was supported by the Department of Defense (W81XH-10-2-0003) and NIH Neurobiology of Aging Training Grant (T32 AG020494) (UNT Health Science Center). Technical support and experimental assistance by Dr. Sauymendra Sarkar is greatly appreciated. We would especially like to thank Dr. Ben Barres and his laboratory for training our laboratory in the primary RGC isolation protocol. Special thanks to Dr. Raghu Krishnamoorthy and Dr. Adnan Dibas for helpful discussions.

References

Alvarez, Maubecin, V., Sanchez, V.N., Rosato Siri, M.D., Cherksey, B.D., Sugimori, M., Llinás, R., Uchitel, O.D., 1995. Pharmacological characterization of the voltage-dependent Ca^{2+} channels present in synaptosomes from rat and chicken central nervous system. J. Neurochem. 64 (6), 2544–2551.

Aydar, E., Palmer, C.P., Klyachko, V.A., Jackson, M.B., 2002. The sigma receptor as a ligand-regulated auxiliary potassium channel subunit. Neuron 34 (3), 399–410.

Barres, B.A., Silverstein, B.E., Corey, D.P., Chun, L.L., 1988. Neuronimmunological, morphological, and electrophysiological variation among retinal ganglion cells purified by panning. Neuron 1 (9), 791–803.

Christopherson, K.S., Ullian, E.M., Stokes, C.C., Mullowney, C.E., Hell, J.W., Agah, A., Lawler, J., Mosher, D.F., Bornstein, P., Barres, B.A., 2005. Thrombospondins are astrocyte-secreted proteins that promote CNS synaptogenesis. Cell. 120 (3), 421–433.

Church, J., Fletcher, E.J., 1995. Blockade by sigma site ligands of high voltage-activated Ca^{2+} channels in rat and mouse cultured hippocampal pyramidal neurons. Br. J. Pharmacol. 116 (7), 2801–2810.

Costes, S.V., Daelemans, D., Cho, E.H., Dobbin, Z., Pavlakis, G., Lockett, S., 2004. Automatic and quantitative measurement of protein-protein colocalization in live cells. Biophys. J. 86 (6), 3993–4003.

Crosson, C.E., Willis, J.A., Potter, D.E., 1990. Effect of the calcium antagonist, nifedipine, on ischemic retinal dysfunction. J. Ocul. Pharmacol. 6 (4), 293–299.

González, L.G., Sánchez-Fernández, C., Cobos, E.J., Baeyens, J.M., del Pozo, E., 2012. Sigma-1 receptors do not regulate calcium influx through voltage-dependent calcium channels in mouse brain synaptosomes. Eur. J. Pharmacol. 677 (1–3), 102–106.

Grynkiewicz, G., Poenie, M., Tsien, R.Y., 1985. A new generation of Ca^{2+} indicators with greatly improved fluorescence properties. J. Biol. Chem. 260 (6), 3440–3450.

Hanner, M., Moebius, F.F., Flandorfer, A., Knaus, H.G., Striessnig, J., Kempner, E., Glossmann, H., 23 1996. Purification, molecular cloning, and expression of the mammalian sigma1-binding site. Proc. Natl. Acad. Sci. U S A 93 (15), 8072–8077.

Hayashi, T., Su, T.P., 2003. Intracellular dynamics of sigma-1 receptors (sigma(1) binding sites) in NG108–15 cells. J. Pharmacol. Exp. Ther. 306 (2), 726–733.

Hayashi, T., Su, T., 2005. The sigma receptor: evolution of the concept in neuropsychopharmacology. Curr. Neuropharmacol. 3 (4), 267–280.

Hayashi, T., Maurice, T., Su, T.P., 2000. Ca^{2+} signaling via σ1 receptors: novel regulatory mechanism affecting intracellular Ca^{2+} concentration. J. Pharmacol. Exp. Ther. 293 (3), 788–798.

Hirooka, K., Kelly, M.E., Baldridge, W.H., Barnes, S., 2000. Suppressive actions of betaxolol on ionic currents in retinal ganglion cells may explain its neuroprotective effects. Exp. Eye Res. 70 (5), 611–621.

Kankaanpää, P., Pahajoki, K., Marjomäki, V., Heino, J., White, D., 2006. BioImageXD. on World Wide Web. http://www.bioimagexd.net.

Kekuda, R., Prasad, P.D., Fei, Y.J., Leibach, F.H., Ganapathy, V., 1996. Cloning and functional expression of the human type 1 sigma receptor (hSigmaR1). Biochem. Biophys. Res. Commun. 229 (2), 553–558.

Lupardus, P.J., Wilke, R.A., Aydar, E., Palmer, C.P., Chen, Y., Ruoho, A.E., Jackson, M.B., 2000. Membrane-delimited coupling between sigma receptors and K^+ channels in rat neurohypophysial terminals requires neither G-protein nor ATP. J. Physiol. 526 (Pt 3), 527–539.

Manders, E.M.M., Verbeek, F.J., Aten, J.A., 1993. Measurement of co-localization of objects in dual-colour confocal images. J. Microsc. 169, 375–382.

Martin, W.R., Eades, C.G., Thompson, J.A., Huppler, R.E., Gilbert, P.E., 1976. The effects of morphine- and nalorphine-like drugs in the nondependent and morphine-dependent chronic spinal dog. J. Pharmacol. Exp. Ther. 197 (3), 517–532.

Maurice, T., Su, T.P., 2009. The pharmacology of sigma-1 receptors. Pharmacol. Ther. 124 (2), 195–206.

Meder, W., Fink, K., Gothert, M., 1997. Involvement of different calcium channels in K^+- and veratridine-induced increases of cytosolic calcium concentration in rat cerebral cortical synaptosomes. Naunyn Schmiedebergs Arch. Pharmacol. 356 (6), 797–805.

Meyer, Franke A., Kaplan, M.R., Pfrieger, F.W., Barres, B.A., 1995. Characterization of the signaling interactions that promote the survival and growth of developing retinal ganglion cells in culture. Neuron 15 (4), 805–819.

Meyer, D.A., Carta, M., Partridge, L.D., Covey, D.F., Valenzuela, C.F., 2002. Neurosteroids enhance spontaneous glutamate release in hippocampal neurons. Possible role of metabotropic sigma1-like receptors. J. Biol. Chem. 277 (32), 28725–28732.

Morin-Surun, M.P., Collin, T., Denavit-Saubie, M., Baulieu, E.E., Monnet, F.P., 1999. Intracellular sigma1 receptor modulates phospholipase C and protein kinase C activities in the brainstem. Proc. Natl. Acad. Sci. U S A 96 (14), 8196–8199.

Myers, A.M., Charifson, P.S., Owens, C.E., Kula, N.S., McPhail, A.T., Baldessarini, R.J., Booth, R.G., Wyrick, S.D., 1994. Conformational analysis, pharmacophore identification, and comparative molecular field analysis of ligands for the neuromodulatory sigma 3 receptor. J. Med. Chem. 37 (24), 4109–4117.

Novakova, M., Ela, C., Bowen, W.D., Hasin, Y., Eilam, Y., 1998. Highly selective sigma receptor ligands elevate inositol 1,4,5-trisphosphate production in rat cardiac myocytes. Eur. J. Pharmacol. 353 (2–3), 315–327.

Prasanna, G., Dibas, A.I., Yorio, T., 2000. Cholinergic and adrenergic modulation of the Ca^{2+} response to endothelin-1 in human ciliary muscle cells. Invest. Ophthalmol. Vis. Sci. 41 (5), 1142–1148.

Quirion, R., Bowen, W.D., Itzhak, Y., Junien, J.L., Musacchio, J.M., Rothman, R.B., Su, T.P., Tam, S.W., Taylor, D.P., 1992. A proposal for the classification of sigma binding sites. Trends Pharmacol. Sci. 13 (3), 85–86.

Seth, P., Leibach, F.H., Ganapathy, V., 1997. Cloning and structural analysis of the cDNA and the gene encoding the murine type 1 sigma receptor. Biochem. Biophys. Res. Commun. 241 (2), 535–540.

Seth, P., Fei, Y.J., Li, H.W., Huang, W., Leibach, F.H., Ganapathy, V., 1998. Cloning and functional characterization of a sigma receptor from rat brain. J. Neurochem. 70 (3), 922–931.

Soriani, O., Foll, F.L., Roman, F., Monnet, F.P., Vaudry, H., Cazin, L., 1999. A-Current down-modulated by sigma receptor in frog pituitary melanotrope cells through a G protein-dependent pathway. J. Pharmacol. Exp. Ther. 289 (1), 321–328.

Su, T.P., Hayashi, T., Vaupel, D.B., 2009. When the endogenous hallucinogenic trace amine N, N-dimethyltryptamine meets the sigma-1 receptor. Science-Signaling 2 (61). pe12.

Tchedre, K.T., Yorio, T., 2008. Sigma-1 receptors protect RGC-5 cells from apoptosis by regulating intracellular calcium, Bax levels, and caspase-3 activation. Invest. Ophthalmol. Vis. Sci. 49 (6), 2577–2588.

Tchedre, K.T., Huang, R.Q., Dibas, A., Krishnamoorthy, R.R., Dillon, G.H., Yorio, T., 2008. Sigma-1 receptor regulation of voltage-gated calcium channels involves a direct interaction. Invest. Ophthalmol. Vis. Sci. 49 (11), 4993–5002.

Toriu, N., Akaike, A., Yasuyoshi, H., Zhang, S., Kashii, S., Honda, Y., Shimazawa, M., Hara, H., 2000. Lomerizine, a Ca^{2+} channel blocker, reduces glutamate-induced neurotoxicity and ischemia/reperfusion damage in rat retina. Exp. Eye Res. 70 (4), 475–484.

Ueda, H., Yoshida, A., Tokuyama, S., Mizuno, K., Maruo, J., Matsuno, K., 2001. Neurosteroids stimulate G protein-coupled sigma receptors in mouse brain synaptic membrane. Neurosci. Res. 41 (1), 33–40.

Ullian, E.M., Sapperstein, S.K., Christopherson, K.S., Barres, B.A., 2001. Control Synapse Number by Glia 291 (5504), 657–661.

Zhang, H., Cuevas, J., 2002. Sigma receptors inhibit high-voltage-activated calcium channels in rat sympathetic and parasympathetic neurons. J. Neurophysiol. 87 (6), 2867–2879.

Zhang, X.J., Liu, L.L., Jiang, S.X., Zhong, Y.M., Yang, X.L., 2011. Activation of the sigma receptor 1 suppresses NMDA responses in rat retinal ganglion cells. Neuroscience 177, 12–22.